Commun. Theor. Phys. **76** (2024) 085403 (6pp) https://doi.org/10.1088/1572-9494/ad4bba

Asymmetric dark matter and Sommerfeld enhancement

Sujuan Qiu, Hoernisa Iminniyaz and Wensheng Huo

School of Physics Science and Technology, Xinjiang University, Urumqi 830017, China

E-mail: wrns@xju.edu.cn

Received 4 March 2024, revised 25 April 2024
Accepted for publication 15 May 2024
Published 4 July 2024

Abstract

We study the relic density of asymmetric dark matter with long-range interactions by considering the Sommerfeld effect. We find that the annihilation cross section of asymmetric dark matter is enhanced by the Sommerfeld effect and thus the relic density is decreased. Then we use the Planck data to constrain the asymmetry factor, coupling, and to derive the upper bounds on the dark matter mass in *s*-wave and *p*-wave annihilation cases.

Keywords: asymmetric dark matter, relic density, Sommerfeld enhancement

(Some figures may appear in colour only in the online journal)

1. Introduction

Recently, a number of models of asymmetric dark matter (DM) have been proposed as an alternative to symmetric DM [1–3]. For asymmetric DM, the particle and antiparticle are not identical [1–3]. Asymmetric DM models offer an effective explanation for the similarity of DM and baryon abundances, $\Omega_{\rm DM} \sim \Omega_{\rm b}$ [4]. In asymmetric DM scenarios, DM is not neutral, rather DM possesses particle–antiparticle asymmetry. In that case, the final abundance is determined not only by the annihilation cross section, but also by the asymmetry factor which is the difference between the particle and antiparticle abundances [5, 6]. The antiparticle abundance is largely depressed to negligible levels when the thermal bath temperature is much lower than the DM mass. The DM abundance in the presence of a particle–antiparticle asymmetry is computed in detail in [5, 6].

In asymmetric DM models, the asymmetric DM is assumed to couple to the light scalar or vector mediators [3, 7–10]. The interaction between the asymmetric DM particles and antiparticles appears as long-range if the mediator is light enough. The wavefunction of a DM particle and antiparticle is distorted by the long-range interaction. It is indeed the Sommerfeld effect [11], which boosts DM annihilation rate at low velocities [12, 13]. The couplings required to obtain the observed DM density through the thermal freeze out mechanism of DM are suppressed due to the Sommerfeld effect [13, 14]. On the other hand, the late-time DM annihilation signals are enhanced for a certain set of couplings [15–22]. Because the Sommerfeld enhancement relies on the coupling of DM to the light force mediator, for the same mass, asymmetric DM needs stronger couplings than symmetric DM, there may be a rather significant effect, phenomenologically, in comparison to the symmetric one.

In [23, 24], the effect of Sommerfeld enhancement on the relic density of asymmetric DM is explored in detail when the light mediator is massless. The authors deduced constraints on the mass and couplings required to obtain the observed value of DM abundance in [23]. Reference [25] discusses the impact of Sommerfeld enhancement on the relic density of asymmetric DM in the case of *s*-wave annihilation when the mediator mass $m_\varphi \neq 0$ in a model-independent way. The authors concluded that the abundance of asymmetric DM is decreased due to the enhancement of the annihilation cross section. In the present work, we consider two minimal cases; in these scenarios, asymmetric DM is coupled to a light vector boson or a light scalar boson. We investigate the effect of Sommerfeld enhancement on the relic density of asymmetric DM for *s*-wave and $p-$ wave annihilations in detail when the mediator mass $m_\varphi \neq 0$, especially the impact of *p*-wave Sommerfeld enhancement on the freeze out of asymmetric DM. We extend our previous analysics in several ways. First, we plot the ratio of asymmetric DM antiparticle abundance to the particle abundance with Sommerfeld enhancement as a function of the inverse-scaled temperature. We find the antiparticle abundance is depleted faster while the annihilation cross section is enhanced by the Sommerfeld effect. The decrease of the ratio is significant for stronger couplings. We

calculate the couplings required to attain the observed DM relic density as a function of the asymmetry factor. The coupling is stronger for asymmetric DM than the symmetric one. The final abundance is largely determined by the asymmetry. When the asymmetry is large, the required mass bound is smaller. In the asymmetric DM case, we also noticed that the maximum value of the mass needed to satisfy the observed value of DM abundance is smaller than the symmetric DM. In our work, we ignored the effect of bound state formation on the relic density of asymmetric DM which affects the relic density of DM only around the unitarity bound [10, 14].

The paper is arranged as follows. In section 2), we discuss the impact of the Sommerfeld effect on the relic abundance of asymmetric DM for *s-0* wave and *p*-wave annihilations when the mediator mass $m_{\varphi} \neq 0$. In section 3, we find constraints on the parameter spaces, such as coupling strength, mass and asymmetry factor when the annihilation cross section of asymmetric DM is modified by the Sommerfeld enhancement. The conclusion and summaries are in the last section.

2. Relic abundance of asymmetric DM including Sommerfeld enhancement

We discuss the effect of Sommerfeld enhancement on the relic density of asymmetric DM in this section. The number density of asymmetric DM particle χ (antiparticle $\bar{\chi}$) is evolved according to the following Boltzmann equation,

$$\frac{\mathrm{d}n_{\chi(\bar{\chi})}}{\mathrm{d}t} + 3Hn_{\chi(\bar{\chi})} = -\langle\sigma v\rangle(n_{\chi}n_{\bar{\chi}} - n_{\chi,\mathrm{eq}}n_{\bar{\chi},\mathrm{eq}}), \tag{1}$$

where $H = \pi T^2/M_{\mathrm{Pl}}\sqrt{g_*/90}$ is the expansion rate of the universe in the radiation dominated era, here $M_{\mathrm{Pl}} = 2.4 \times 10^{18}$ GeV is the reduced Planck mass, and g_* being the effective number of relativistic degrees of freedom. The equilibrium number densities are $n_{\chi(\bar{\chi}),\mathrm{eq}} = g_{\chi}[mT/(2\pi)]^{3/2}\mathrm{e}^{(-m\pm\mu_{\chi})/T}$, where g_{χ} is the number of the intrinsic degrees of freedom of the particle. Here, the chemical potentials $\mu_{\bar{\chi}} = -\mu_{\chi}$ when the asymmetric DM is in equilibrium state. The thermally-averaged Sommerfeld enhanced annihilation cross section is

$$\langle\sigma\ v\rangle = a\ \langle S_s\rangle + b\ \langle v^2\ S_p\rangle. \tag{2}$$

Here a is the $s-$wave contribution when $v \to 0$ and b is the p-wave contribution when the $s-$wave is suppressed. The Sommerfeld enhancement factors for the massive mediator in the case of *s*-wave and *p*-wave annihilations are given in [26–29]. For $s-$wave annihilation,

$$S_s = \frac{2\pi\alpha}{v}\frac{\sinh\left(\frac{6mv}{\pi m_{\phi}}\right)}{\cosh\left(\frac{6mv}{\pi m_{\phi}}\right) - \cos\left(2\pi\sqrt{\frac{6\alpha m}{\pi^2 m_{\phi}} - \frac{9m^2v^2}{\pi^4 m_{\phi}^2}}\right)}, \tag{3}$$

where v is the relative velocity of the annihilating asymmetric DM particle χ and antiparticle $\bar{\chi}$, and α is the coupling strength. For p-wave annihilation, the Sommerfeld enhancement factor is

$$S_p = \frac{(6\alpha m/(\pi^2 m_{\phi}) - 1)^2 + 36m^2v^2/(\pi^4 m_{\phi}^2)}{1 + 36m^2v^2/(\pi^4 m_{\phi}^2)}\,S_s. \tag{4}$$

Then

$$\langle S_s\rangle = \frac{x^{3/2}}{2\sqrt{\pi}}\int_0^{\infty} v^2\,\mathrm{e}^{-\frac{x}{4}v^2}\,S_s\,\mathrm{d}v. \tag{5}$$

$$\langle v^2\,S_p\rangle = \frac{x^{3/2}}{2\sqrt{\pi}}\int_0^{\infty} v^4\,\mathrm{e}^{-\frac{x}{4}v^2}\,S_p\,\mathrm{d}v. \tag{6}$$

For convenience, equation (1) can be expressed in terms of $Y_{\chi(\bar{\chi})} = n_{\chi(\bar{\chi})}/s$, and $x = m/T$; here $s = 2\pi^2 g_{*s}/45\,T^3$ is the entropy density with g_{*s} being the effective number of entropic degrees of freedom. Here, we assume the Universe expands adiabatically and the entropy is conserved per comoving volume, then equation (1) becomes

$$\frac{\mathrm{d}Y_{\chi(\bar{\chi})}}{\mathrm{d}\,x} = -\frac{\lambda\langle\sigma v\rangle}{x^2}(Y_{\chi}\,Y_{\bar{\chi}} - Y_{\chi,\mathrm{eq}}\,Y_{\bar{\chi},\mathrm{eq}}), \tag{7}$$

where $\lambda = 1.32\,mM_{\mathrm{Pl}}\sqrt{g_*}$, $g_* \simeq g_{*s}$ and $\mathrm{d}g_{*s}/\mathrm{d}x \simeq 0$.

By subtracting the Boltzmann equations for χ and $\bar{\chi}$ in equation (7), we obtain $Y_{\chi} - Y_{\bar{\chi}} = \eta$, where η is a constant. Then the Boltzmann equation (7) is rewritten as

$$\frac{\mathrm{d}Y_{\chi(\bar{\chi})}}{\mathrm{d}\,x} = -\frac{\lambda\langle\sigma v\rangle}{x^2}(Y_{\chi(\bar{\chi})}^2 \mp \eta Y_{\chi(\bar{\chi})} - Y_{\mathrm{eq}}^2), \tag{8}$$

here

$$Y_{\mathrm{eq}}^2 = Y_{\chi,\mathrm{eq}}Y_{\bar{\chi},\mathrm{eq}} = (0.145g_{\chi}/g_*)^2\,x^3\mathrm{e}^{-2x}. \tag{9}$$

To solve the Boltzmann equation (8), we follow the standard picture of particle evolution. It is supposed that the asymmetric DM particles and antiparticles were in thermal equilibrium with the standard model particles in the early universe. When the temperature drops as $T < m$ for $m > |\mu_{\chi}|$, the interaction rate Γ falls below the expansion rate H. At this freeze out point, asymmetric DM decouples from the equilibrium state and the number density of asymmetric DM in a comoving space becomes almost constant [5, 6, 30]. Following the method which is used in [6], the final abundance of antiparticles is determined as

$$Y_{\bar{\chi}}(x_{\infty}) = \frac{\eta}{\exp\left[\,1.32\,\eta\,mM_{\mathrm{Pl}}\sqrt{g_*}\int_{\bar{x}_{\mathrm{F}}}^{\infty}\langle\sigma v\rangle/x^2\,\mathrm{d}x\,\right] - 1}, \tag{10}$$

here

$$Y_{\bar{\chi}}(x_{\infty}) \equiv \lim_{x\to\infty} Y_{\bar{\chi}}(x). \tag{11}$$

The freeze out temperature $\bar{x}_{\mathrm{F}}$ is fixed by using the standard procedure which assumes the freeze out occurred at the point when the deviation of the relic abundance $Y_{\bar{\chi}}(\bar{x}_{\mathrm{F}})$ and $Y_{\bar{\chi},\mathrm{eq}}(\bar{x}_{\mathrm{F}})$ is of the same order as the equilibrium value such as $Y_{\bar{\chi}}(\bar{x}_{\mathrm{F}}) = (1+\xi)Y_{\bar{\chi},\mathrm{eq}}(\bar{x}_{\mathrm{F}})$. Here, ξ is a constant and usually we take $\xi = \sqrt{2} - 1$ [30]. The relic abundance of the particle

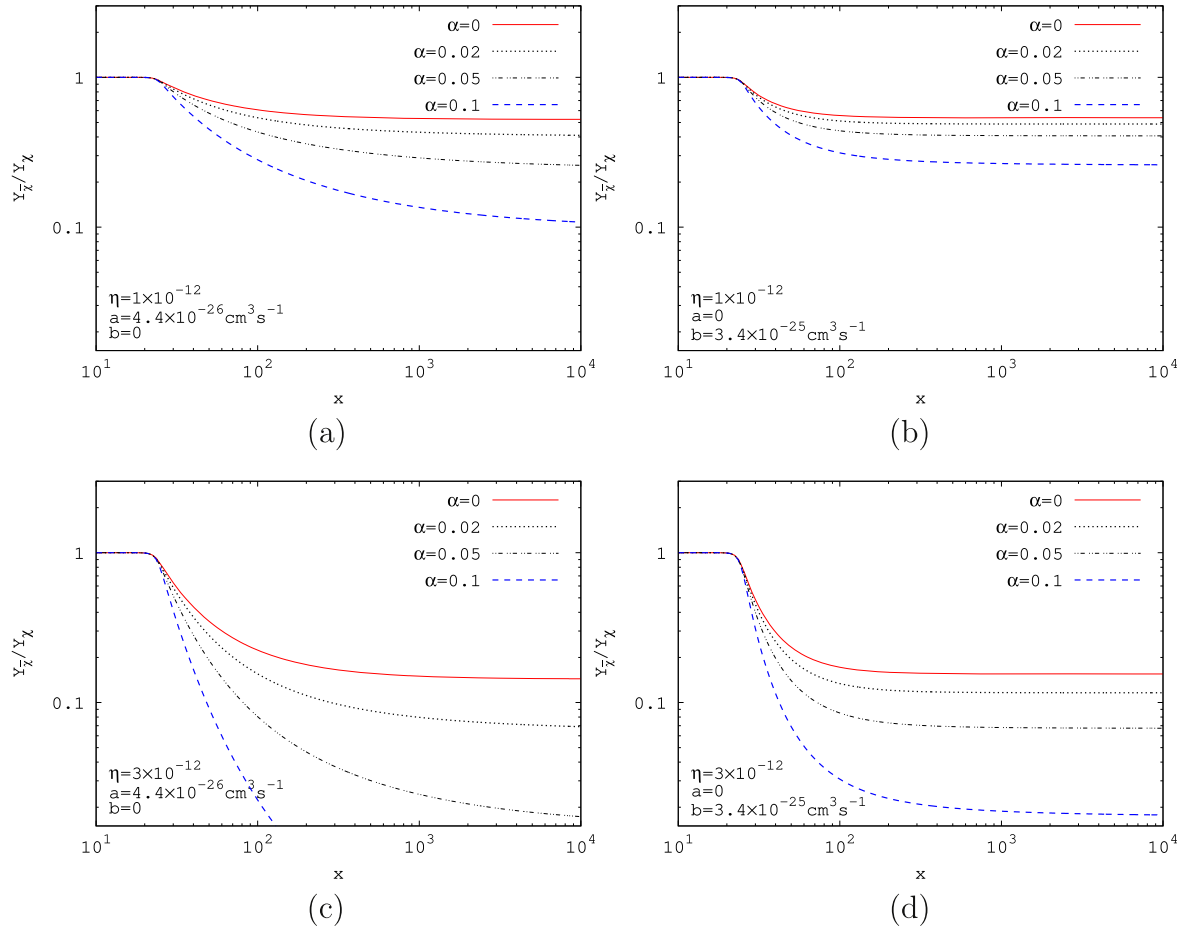

Figure 1. Ratio of the asymmetric DM abundances $Y_{\bar{\chi}}$ and Y_χ as a function of x for the Sommerfeld enhanced annihilation cross section. Here, $m = 130$ GeV, $m_\varphi = 0.25$ GeV, $g_\chi = 2$, $g_* = 90$.

is obtained by using $Y_\chi = Y_{\bar{\chi}} + \eta$,

$$Y_\chi(x_\infty) = \frac{\eta}{1 - \exp\left[-1.32\,\eta\, m M_{\rm Pl}\,\sqrt{g_*}\,\int_{x_{\rm F}}^{\infty}\langle\sigma v\rangle/x^2\,{\rm d}x\right]}, \tag{12}$$

where x_F is the freeze out temperature of χ. Equations (10) and (12) are consistent with the constraint $Y_\chi = Y_{\bar{\chi}} + \eta$ only if $x_{\rm F} = \bar{x}_{\rm F}$. The total final DM relic density is

$$\Omega_{\rm DM}h^2 = 2.76 \times 10^8\, m[Y_\chi(x_\infty) + Y_{\bar{\chi}}(x_\infty)]{\rm GeV}^{-1}, \tag{13}$$

where $\Omega_\chi = \rho_\chi/\rho_c$ with $\rho_\chi = n_\chi m = s_0 Y_\chi$ and $\rho_c = 3H_0^2 M_{\rm Pl}^2$; here $s_0 \simeq 2900$ cm^{-3} is the present entropy density, and H_0 is the Hubble constant. Figure 1 shows the ratio of the antiparticle abundance $Y_{\bar{\chi}}$ to the particle abundance Y_χ as a function of the inverse-scaled temperature x for the Sommerfeld enhanced annihilation cross section. It is based on the numerical solutions of equation (8). Here, panels (a) and (c) are for the s-wave annihilation, panels (b) and (d) are for p-wave annihilation. The particle and antiparticle abundances are the same amount before the decoupling from the equilibrium state. After freeze out, asymmetric DM abundances become almost constant, which is shown in the figure. We find that the effect of Sommerfeld enhancement is significant for the stronger coupling α and for the larger asymmetry factor η. In other words, the depletion of antiparticle abundance is faster when α is large. For p-wave annihilation, the decrease of the antiparticle abundance is slower than s-wave annihilation.

3. Constraints

In this section, we discuss two minimal cases in which the asymmetric DM couples to a light vector or scalar boson. In the case of the vector mediator, we consider the process $\chi\bar{\chi} \to 2\gamma$ which is discussed in [23]. The Sommerfeld enhanced annihilation cross section times the relative velocity is

$$(\sigma\, v)_{\rm s-wave} = \sigma_0\, S_s, \tag{14}$$

where the annihilation into two vector bosons is an s-wave process and the leading order cross section is $\sigma_0 = \pi\alpha^2/m^2$ [23].

For the scalar mediator, the process $\chi\bar{\chi} \to 2\varphi$ is considered. The annihilation cross section times the relative velocity is given by

$$(\sigma v)_{\rm p-wave} = \sigma_1\, v^2 S_p, \tag{15}$$

where the annihilation of two fermions into two scalar bosons

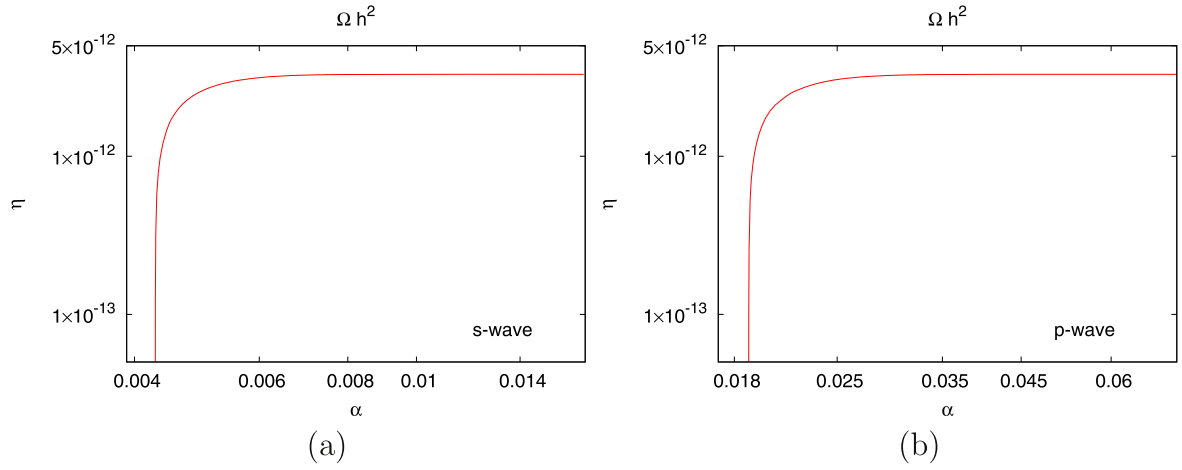

Figure 2. Contour plots of the asymmetry factor η with coupling strength α for s-wave (p-wave) annihilation cross section when $\Omega_{\rm DM}h^2 = 0.120$ [4]. Here, $m = 130$GeV, $m_\varphi = 0.25$ GeV, $g_\chi = 2$, $g_* = 90$.

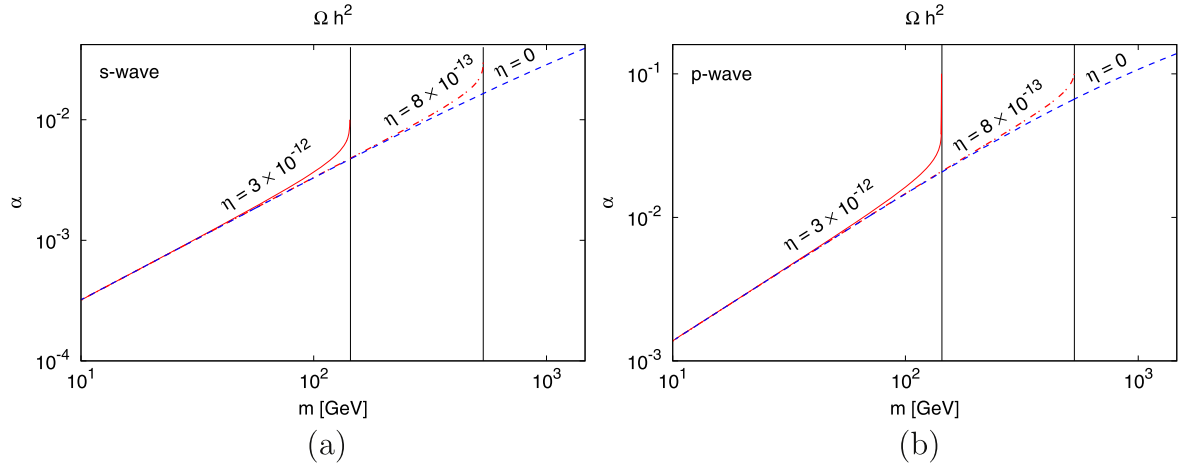

Figure 3. Contour plots of coupling strength α and mass m for s-wave (p-wave) annihilation when $\Omega_{\rm DM}h^2 = 0.120$ [4]. Here, $m_\varphi = 0.25$ GeV, $g_\chi = 2$, $g_* = 90$, where σ_0 and σ_1 are evaluated by using the correlated α.

is a p-wave process and the tree level cross section is $\sigma_1 = 3\pi\alpha^2/(8{\rm m}^2)$ [23].

In the following, we insert equations (14) and (15) into equation (8) separately and using Planck data to find constraints on the coupling strength α, asymmetry factor η and mass m. In figure 2, the relation between the asymmetry factor η and the coupling strength α for s-wave (p-wave) annihilation is shown when $\Omega_{\rm DM}h^2 = 0.120$ [4]. Here, σ_0 and σ_1 are evaluated by using the correlated α. The abundance is not sensitive to the smaller value of η. When η is small, the symmetric case is recovered. Therefore, the contour line climbs vertically (countours are independent of η). On the other hand, the smaller η gives the minimal allowed value of the coupling strengths $\alpha = 0.0043$ for s-wave and $\alpha = 0.0188$ for p-wave annihilations. The lower bound of α is larger for p-wave annihilation. The curves flatten out rapidly while the asymmetry η is increased. The relic abundance is determined by the asymmetry. In that case, the abundance is not affected when the coupling strength is increased (independent of α). A stronger coupling α corresponds to the greater enhancement of the cross section. It leads to a smaller relic density. This should be compensated by increasing η.

The coupling strength required to obtain the observed value of DM relic density with mass is plotted in figure 3. The mass bounds for $\eta = 3 \times 10^{-12}$, 8×10^{-13} are $m = 143$, 535 GeV respectively in panel (a); $m = 143$, 532 GeV in panel (b). Highly asymmetric DM has a lower mass bound. For the same mass bound, asymmetric DM needs stronger coupling to attain the observed value of DM relic density in comparison to the symmetric case. For example, when $m = 143$ GeV, the coupling strengths $\alpha = 0.01$ for $\eta = 3 \times 10^{-12}$ and $\alpha = 0.005$ for $\eta = 0$. The value of the coupling for s-wave annihilation is smaller than the case of p-wave annihilation.

The contour plots of the cross section with mass are shown in figure 4 when $\Omega_{\rm DM}h^2 = 0.120$. The allowed region is bounded by the cross section from below and by the maximum value of mass from the right for different asymmetry factors η. For $m \ll m_{\rm max}$, the coupling constant α and $\sigma_0(\sigma_1)$ trace the symmetric DM ($\eta = 0$) case closely. When the cross section is small, the abundance is insensitive to the increased mass. On the other hand, while α is small, the effect of Sommerfeld enhancement is not significant both for the symmetric and asymmetric DM. As the mass is reached, the

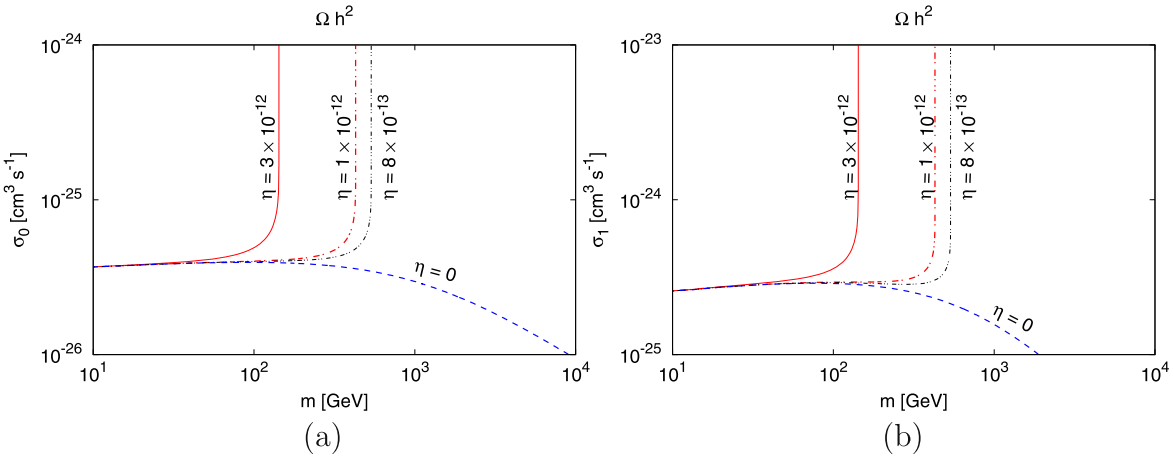

Figure 4. Contour plots of s-wave (p-wave) annihilation cross section $\sigma_0(\sigma_1)$ and mass when $\Omega_{\rm DM}h^2 = 0.120$. Here, $m_\phi = 0.25$ GeV, $g_\chi = 2$, $g_* = 90$; the coupling α is computed by using the expression $\sigma_0 = \pi\alpha^2/m^2$ for s-wave and $\sigma_1 = 3\pi\alpha^2/(8m^2)$ for p-wave annihilations.

maximum value $m \simeq m_{\rm max}$, the Sommerfeld enhanced annihilation cross section is increased to satisfy the observed value of the DM relic density for asymmetric DM. In the symmetric case, the coupling is stronger for larger m (see figure 3). Then, the Sommerfeld enhanced cross section reduces the relic density notably, thus the cross section should be small in order to obtain the required value of the relic density. Therefore, the cross section falls quickly when the mass is increased in the symmetric case.

4. Summary and conclusions

When the asymmetric DM is coupled to the light force carrier, the annihilation cross section is enhanced by the Sommerfeld effect. We discuss the impact of Sommerfeld enhancement on the relic density of asymmetric DM for $s-$wave and $p-$wave annihilations for the case of light mediator $m_\varphi \neq 0$ in detail. We found that the antiparticle abundance is depleted faster than the standard case due to the Sommerfeld enhanced annihilation cross section. The decrease in the ratio of antiparticle abundance to particle abundance is notable for the stronger coupling α.

We apply our method to two kinds of scenarios in which asymmetric DM couples to either the light vector mediator or the scalar mediator. Using the Planck data, we constrain the coupling strength α, asymmetry factor η and the mass value m. When η is small, the abundance is independent of η, and it is indeed the symmetric case. The minimal values of the coupling strength are $\alpha = 0.0043$ for s-wave and $\alpha = 0.0188$ for p-wave annihilations. When η takes a larger value, the relic abundance is determined by the asymmetry and it is independent of α. For the same mass bound $m_{\rm max}$, asymmetric DM needs stronger coupling to attain the observed value of DM relic density in comparison to the symmetric case. When the cross section is small, the abundance is insensitive to the increased mass. While the mass reached the maximum value, the Sommerfeld enhanced annihilation cross section is increased to satisfy the observed value of the DM relic density.

Our results are important when the effect of Sommerfeld enhancement is significant at low velocity limit. The Sommerfeld effect hints at notable indirect detection signals from the asymmetric DM antiparticle. This allows us to examine the asymmetric DM by the cosmic microwave background observation, the Milky Way and dwarf galaxies.

Acknowledgments

The work is supported by the National Natural Science Foundation of China (U2031204, 11 765 021) and Natural Science Foundation of Xinjiang Uygur Autonomous Region (2022D01C52).

References

[1] Griest K and Seckel D 1987 Cosmic asymmetry, neutrinos and the sun *Nucl. Phys.* B **283** 681
Hooper D, March-Russell J and West S M 2005 Asymmetric sneutrino Dark Matter and the $\Omega_{\rm b}/\Omega_{\rm DM}$ puzzle *Phys. Lett.*B **605** 228
An H, Chen S L, Mohapatra R N and Zhang Y 2010 Leptogenesis as a common origin for matter and dark matter *J. High Energy Phys.* JHEP03(2010)124
Cohen T and Zurek K M 2010 Leptophilic dark matter from the lepton asymmetry *Phys. Rev. Lett.* **104** 101301
Kaplan D E, Luty M A and Zurek K M 2009 Asymmetric dark matter *Phys. Rev.* D **79** 115016
Cohen T, Phalen D J, Pierce A and Zurek K M 2010 Asymmetric dark matter from a GeV hidden sector *Phys. Rev.* D **82** 056001
Shelton J and Zurek K M 2010 Darkogenesis: a baryon asymmetry from the Dark Matter sector *Phys. Rev.* D **82** 123512
[2] Belyaev A, Frandsen M T, Sarkar S and Sannino F 2011 Mixed dark matter from technicolor *Phys. Rev.* D **83** 015007
[3] Petraki K, Pearce L and Kusenko A 2014 Self-interacting asymmetric dark matter coupled to a light massive dark photon *J. Cosmol. Astropart. Phys.* JCAP07(2014)039
[4] Aghanim N *et al* (Planck) 2020 Planck 2018 results. VI. Cosmological parameters *Astron. Astrophys.* **641** A6 [erratum: Astron. Astrophys. **652** (2021), C4]

[5] Graesser M L, Shoemaker I M and Vecchi L 2011 Asymmetric WIMP dark matter *J. High Energy Phys.* JHEP10(2011)110
[6] Iminniyaz H, Drees M and Chen X 2011 Relic abundance of asymmetric dark matter *J. Cosmol. Astropart. Phys.* JCAP07 (2011)003
[7] Feng J L, Kaplinghat M, Tu H and Yu H B 2009 Hidden charged dark matter *J. Cosmol. Astropart. Phys.* JCAP07 (2009)004
[8] Agrawal P, Cyr-Racine F Y, Randall L and Scholtz J 2017 Dark catalysis *J. Cosmol. Astropart. Phys.* JCAP08 (2017)021
[9] Agrawal P, Cyr-Racine F Y, Randall L and Scholtz J 2017 Make dark matter charged again *J. Cosmol. Astropart. Phys.* JCAP05(2017)022
[10] Cirelli M, Panci P, Petraki K, Sala F and Taoso M 2017 Dark Matter's secret liaisons: phenomenology of a dark U(1) sector with bound states *J. Cosmol. Astropart. Phys.* JCAP05(2017)036
[11] Sommerfeld A 1931 Über die beugung und bremsung der elektronen *Ann. Phys.* **403** 257–330
[12] Hisano J, Matsumoto S and Nojiri M M 2003 Unitarity and higher order corrections in neutralino dark matter annihilation into two photons *Phys. Rev.* D **67** 075014
[13] Hisano J, Matsumoto S and Nojiri M M 2004 Explosive dark matter annihilation *Phys. Rev. Lett.* **92** 031303
[14] von Harling B and Petraki K 2014 Bound-state formation for thermal relic dark matter and unitarity *J. Cosmol. Astropart. Phys.* JCAP12(2014)033
[15] Pospelov M and Ritz A 2009 Astrophysical signatures of secluded dark matter *Phys. Lett.* B **671** 391–7
[16] March-Russell J D and West S M 2009 WIMPonium and boost factors for indirect dark matter detection *Phys. Lett.* B **676** 133–9
[17] Petraki K, Postma M and de Vries J 2017 Radiative bound-state-formation cross-sections for dark matter interacting via a Yukawa potential *J. High Energy Phys.* JHEP04(2017)077
[18] Hisano J, Matsumoto S, Nojiri M M and Saito O 2005 Non-perturbative effect on dark matter annihilation and gamma ray signature from galactic center *Phys. Rev.* D **71** 063528
[19] Arkani-Hamed N, Finkbeiner D P, Slatyer T R and Weiner N 2009 A theory of dark matter *Phys. Rev.* D **79** 015014
[20] An H, Wise M B and Zhang Y 2016 Effects of bound states on dark matter annihilation *Phys. Rev.* D **93** 115020
[21] An H, Wise M B and Zhang Y 2017 Strong CMB constraint on p-wave annihilating dark matter *Phys. Lett.* B **773** 121–4
[22] Bringmann T, Kahlhoefer F, Schmidt-Hoberg K and Walia P 2017 Strong constraints on self-interacting dark matter with light mediators *Phys. Rev. Lett.* **118** 141802
[23] Baldes I and Petraki K 2017 Asymmetric thermal-relic dark matter: sommerfeld-enhanced freeze-out, annihilation signals and unitarity bounds *J. Cosmol. Astropart. Phys.* JCAP09(2017)028
[24] Abudurusuli A and Iminniyaz H Relic density of asymmetric dark matter with Sommerfeld enhancement accepted (arXiv:2001.08404)
[25] Sulitan A, Iminniyaz H and Baoxia M 2021 Sommerfeld enhancements for asymmetric dark matter *Chin. J. Phys.* **70** 117–24
[26] Kamada A, Kim H J and Kuwahara T 2020 Maximally self-interacting dark matter: models and predictions *J. High Energy Phys.* JHEP12(2020)202
[27] Duerr M, Schmidt-Hoberg K and Wild S 2018 Self-interacting dark matter with a stable vector mediator *J. Cosmol. Astropart. Phys.* JCAP09(2018)033
[28] Feng J L, Kaplinghat M and Yu H B 2010 Sommerfeld enhancements for thermal relic dark matter *Phys. Rev.* D **82** 083525
[29] Cassel S 2010 Sommerfeld factor for arbitrary partial wave processes *J. Phys.* G **37** 105009
[30] Scherrer R J and Turner M S 1986 On the relic, cosmic abundance of stable, weakly interacting massive particles *Phys. Rev.* D **33** 1585
Scherrer R J and Turner M S 1986 On the relic, cosmic abundance of stable, weakly interacting massive particles *Phys. Rev.* D **34** 3263